Diffraction of acoustic waves at two-dimensional hard trilateral cylinders with rounded edges: First-order physical theory of diffraction approximation

Gokhan Apaydin,[1,a)] Levent Sevgi,[2] and Pyotr Ya. Ufimtsev[3]
[1]*Department of Electrical and Electronics Engineering, Uskudar University, Istanbul 34662, Turkey*
[2]*Department of Electrical and Electronics Engineering, Okan University, Tuzla Campus, Akfirat, Istanbul 34959, Turkey*
[3]*EM Consulting, 1959 Barry Avenue, Los Angeles, California 90025, USA*

(Received 26 January 2018; revised 5 April 2018; accepted 20 April 2018; published online 9 May 2018)

The paper explores diffraction of acoustic waves at a two-dimensional hard trilateral cylinder with rounded edges. It represents the extension of the physical theory of diffraction (PTD) for finite objects with rounded edges. A first-order PTD approximation is developed. Integral equations are formulated for acoustic fringe waves and solved by method of moments (MoM). Good agreement is observed with the exact solution found by MoM when the object size exceeds a few wavelengths.
 https://doi.org/10.1121/1.5037096

[DDE] Pages: 2792–2795

I. INTRODUCTION

The paper extends the physical theory of diffraction (PTD) for finite objects with rounded edges. It started recently for objects with soft boundaries (Apaydin *et al.*, 2017b). Here, we consider diffraction of acoustic waves at a hard trilateral cylinder. Notice that this two-dimensional acoustic problem admits electromagnetic interpretation. It is diffraction at a perfectly conducting object illuminated by a plane wave with its magnetic field vector parallel to the z-axis (Fig. 1). The acoustic surface velocity potential u can be treated as the surface electric current j (Ufimtsev, 1989, 2006, 2014). This current terminology is used in the paper. More information about PTD can be found in Ufimtsev (2013, 2009, 2014). See also the recent PTD applications for finite wedges (Rozynova and Xiang, 2017; Xiang and Rozynova, 2017). Notice as well the theoretical (Apaydin *et al.*, 2017b) and empirical (Chambers and Berthelot, 1994) studies of sharp edges vs rounded edges.

The fundamental idea of PTD is a separation of the surface currents in two components, $j = j^{\mathrm{PO}} + j^{\mathrm{fr}}$ (Ufimtsev, 1989, 2014). The first one is the usual physical optics (PO) approximation while the second represents the diffraction/fringe component caused by the curvature of the object surface. This component is found via solving the surface fringe integral equations (Apaydin *et al.*, 2016b; Apaydin *et al.*, 2017a) by the method of moments (MoM). Alternative approaches in the theory of diffraction at rounded objects and polygonal cylinders are presented in Elsherbeni and Hamid (1985), Hallidy (1985), Hamid (1973), Lucido *et al.* (2006), Mitzner *et al.* (1990), Vasiliev *et al.* (1991), and Yarmakhov (2004).

The paper is organized as follows: Sec. II describes the geometry of the problem. In Sec. III, the integral equations for the acoustic fringe currents are formulated. Section IV presents numerical simulations.

The time dependence $\exp(-i\omega t)$ is used in the paper.

II. GEOMETRY OF THE PROBLEM

We investigate diffraction of acoustic waves at a hard equilateral cylinder with sections $L_1 = L_2 = L_3$ shown in Fig. 1 under the boundary condition $\partial u/\partial n = 0$. The cylinder is illuminated by the incident plane wave

$$u^{\mathrm{inc}} = e^{ikx}. \tag{1}$$

Sections L_{01}, L_{02}, L_{03} are parts of circular cylinders with radius a. They are smoothly conjugated with the faces of the tangential wedges. Points 1, 2, and 3 denote the tips of these wedges. The angle between faces equals to $2\beta = \pi/3$, that is $\beta = \pi/6$.

III. FORMULATION OF THE PROBLEM

In a high-frequency situation, when the acoustic wavelength is very small compared to the distance between edges, one can neglect the multiple diffracted edge waves. In this case, the acoustic fringe currents j^{fr} in the vicinity of the object edges are asymptotically identical to those on the rounded tangential wedges with the same shape of the edge and with infinite faces. We call them primary (single-diffracted) currents and focus on their calculation. Denote these currents as $j_1^{fr}, j_2^{fr}, j_3^{fr}$ for the wedges whose extended faces intersect each other at points 1, 2, 3, respectively. To calculate them, we apply the fringe integral equations introduced in Apaydin *et al.* (2016b). They are reproduced here briefly,

$$\frac{1}{2} j^{\mathrm{fr}}(x,y) - \frac{i}{4}\,\mathrm{p.v.}\int_L j^{\mathrm{fr}}(x',y')\,\frac{\partial}{\partial n} H_0^{(1)}(kr)\,dl' = \frac{i}{4}\,\mathrm{p.v.}\int_L j^{\mathrm{PO}}(x',y')\,\frac{\partial}{\partial n} H_0^{(1)}(kr)\,dl' \tag{2}$$

a)Electronic mail: gokhan.apaydin@uskudar.edu.tr

 0001-4966/2018/143(5)/2792/4/$30.00

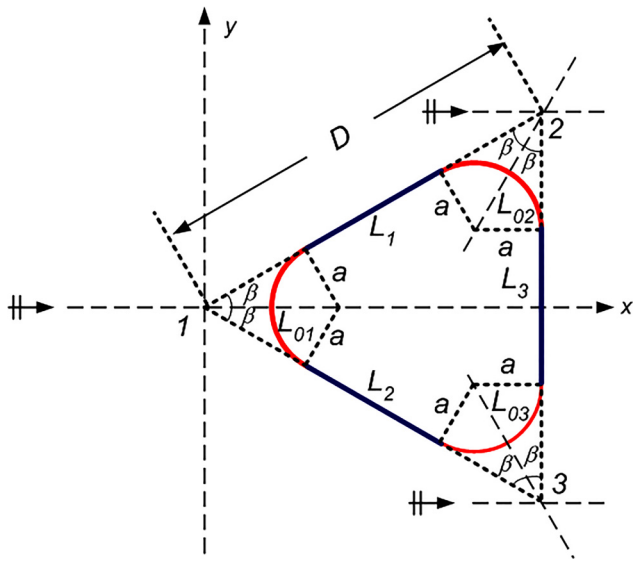

FIG. 1. (Color online) Cross-section of the scattering hard object. Sections L_{01}, L_{02}, L_{03} are parts of the circular cylinders with radius a, the length of sections L_1, L_2, L_3 is L, $D = 2a\cot\beta + L$, $\beta = \pi/6$.

for the illuminated side L^{ill} and

$$\frac{1}{2}j^{\text{fr}}(x,y) - \frac{i}{4}\text{p.v.}\int_L j^{fr}(x',y')\frac{\partial}{\partial n}H_0^{(1)}(kr)dl' = u^{\text{inc}}(x,y) + \frac{i}{4}\text{p.v.}\int_L j^{\text{PO}}(x',y')\frac{\partial}{\partial n}H_0^{(1)}(kr)dl' \quad (3)$$

for the shadowed side L^{sh}. Here, $L>0$ and $dl' \geq 0$. The symbol p.v. $\int$ means the Cauchy principal value of the integral. The integral terms on the right-hand side of Eqs. (2) and (3) represent the PO acoustic field. Equations (2) and (3) can be solved by the classic MoM (Harrington, 1993). Actually, we need to solve three sets of integral equations associated with three tangential wedges:

- the wedge with $L = L_{01} + L_1 + L_2$,
- the wedge with $L = L_{02} + L_1 + L_3$,
- the wedge with $L = L_{03} + L_3 + L_2$,

where L_1, L_2, L_3 formally are infinitely long, but during practical calculation, they have been set to equal $L_1 = L_2 = L_3 = L$ (Fig. 1) and finite. It was established that this assumption is effective already in the case when $L \geq 3\lambda$ (Ufimtsev, 2014).

Denote the acoustic fringe currents on the rounded tangential wedges as $j_1^{\text{fr}}, j_2^{\text{fr}}, j_3^{\text{fr}}$, respectively. The total fringe current on the actual object is the sum

$$j^{\text{fr,PTD}} = j_1^{\text{fr}} + j_2^{\text{fr}} + j_3^{\text{fr}}. \quad (4)$$

Solving Eqs. (2) and (3), the fringe current Eq. (4) is obtained.

To test/validate this PTD approximation, the exact fringe current has been calculated as the difference:

$$j^{\text{fr,exact}} = j^{\text{tot,exact}} - j^{\text{PO}}. \quad (5)$$

Here $j^{\text{tot,exact}}$ is found by solving the integral equation for the actual total current on the object:

$$\frac{1}{2}j^{\text{tot}}(x,y) - \frac{i}{4}\text{p.v.}\int_L j^{tot}(x',y')\frac{\partial}{\partial n}H_0^{(1)}(kr)dl' = u^{\text{inc}}(x,y) \quad (6)$$

that includes all multiple fringe waves/currents. The acoustic fields generated by the surface currents are calculated as

$$u(x,y) = \frac{i}{4}\int_L j(x',y')\frac{\partial}{\partial n}H_0^{(1)}(kr)dl'. \quad (7)$$

The currents in Eqs. (4) and (5) and the acoustic fields generated by them are indicated in Figs. 2–6 by labels PTD and MoM, respectively. The MoM data are considered to be exact.

Notice that in Figs. 3–6 we plot the normalized acoustic scattering cross-section σ_{norm} defined by (5.45) in Ufimtsev (2014) with $l = 2a + L$. Equations (2), (3), and (6) have been solved numerically by MoM. Examples of its applications to fringe integral equations are given in Apaydin *et al.* (2016a) and Apaydin and Sevgi (2016).

The MoM has been used in scattering and diffraction modeling (Apaydin *et al.*, 2014; Uslu *et al.*, 2014). In this method, the object under investigation is discretized and replaced with a number of neighboring segments. The segment lengths are specified according to the wave frequency. As a rough criterion, the length of each segment should be equal to one-hundredth of the wavelength for discretization in almost all frequency and time domain models (this is a rough discretization; depending on the problem at hand as many as several dozen segments may be required).

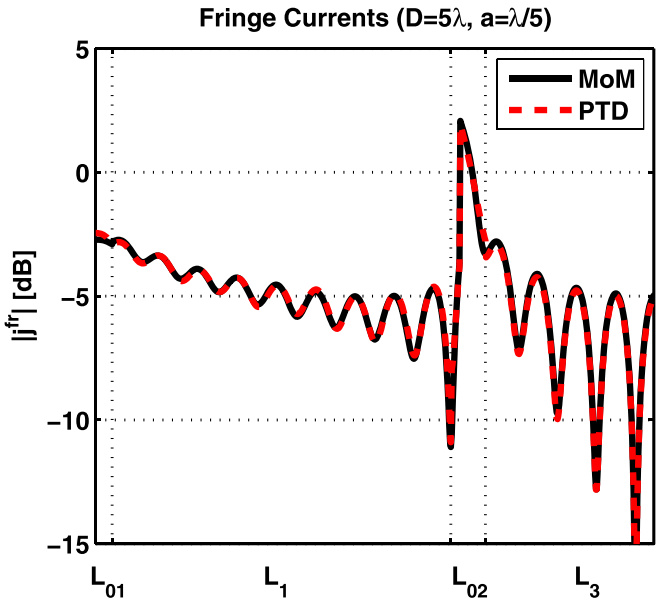

FIG. 2. (Color online) Acoustic fringe waves/currents induced on the upper surface ($y \geq 0$) of the hard rounded trilateral cylinder ($a = \lambda/5$, $D = 5\lambda$, $dl \cong \lambda/100$, $N_{L_{01}} = N_{L_{02}} = N_{L_{03}} = 44$, $N_{L_1} = N_{L_2} = N_{L_3} = 432$).

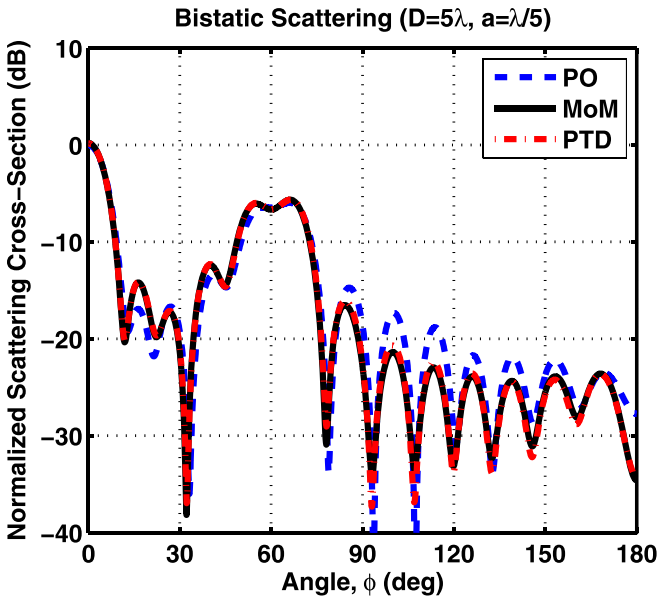

FIG. 3. (Color online) Bistatic scattering of acoustic waves at the hard rounded trilateral cylinder ($a=\lambda/5, D=5\lambda,\ dl\cong\lambda/100,\ N_{L_{01}}=N_{L_{02}}=N_{L_{03}}=44, N_{L_1}=N_{L_2}=N_{L_3}=432$).

IV. NUMERIC SIMULATIONS

Acoustic fringe currents, fringe fields, and scattered acoustic fields are comparatively given in this section. Figure 2 shows fringe currents induced on the upper surface ($y\geq 0$) of the hard rounded trilateral cylinder. Here, solid and dashed curves belong to $|j^{\mathrm{fr,MoM}}|$ and $|j^{\mathrm{fr,PTD}}|$, respectively. The discretization parameters used in the calculations are mentioned in the figure captions. As observed, the agreement is good. The MoM and PTD curves here totally coincide with the graphical resolution.

Notice here the high peak between two conjugation points of the section L_{02} with L_1 and L_3. It is clearly associated with the curvature discontinuities at these points.

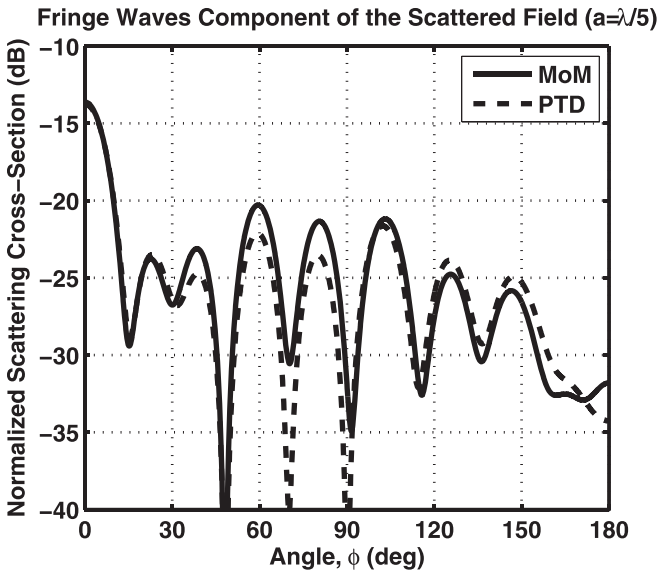

FIG. 4. Acoustic field generated in the far zone by the fringe currents induced on the hard rounded trilateral cylinder ($a=\lambda/5, D=3\lambda,\ dl\cong\lambda/100,\ N_{L_{01}}=N_{L_{02}}=N_{L_{03}}=44, N_{L_1}=N_{L_2}=N_{L_3}=232$).

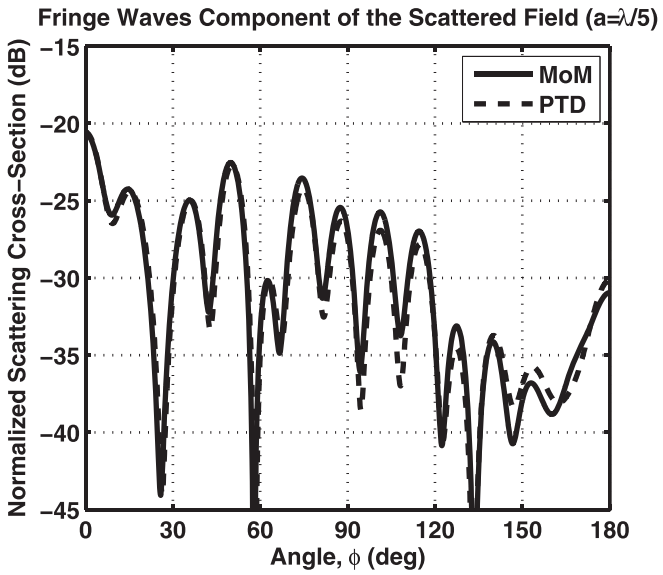

FIG. 5. Acoustic field generated in the far zone by the fringe currents induced on the hard rounded trilateral cylinder ($a=\lambda/5, D=5\lambda,\ dl\cong\lambda/100,\ N_{L_{01}}=N_{L_{02}}=N_{L_{03}}=44, N_{L_1}=N_{L_2}=N_{L_3}=432$).

In the next figures, we plot the normalized acoustic scattering cross-section σ_{norm}. Figure 3 displays the bistatic scattering of acoustic waves at the hard rounded trilateral cylinder for $a=\lambda/5$. Here, dashed, solid, and dashed-dotted curves belong to $\sigma_{\mathrm{norm}}^{\mathrm{PO}}$, $\sigma_{\mathrm{norm}}^{\mathrm{MoM}}$, and $\sigma_{\mathrm{norm}}^{\mathrm{PTD}}$, respectively. As observed, MoM and PTD solutions agree quite well, while PO is insufficient in representing the diffraction phenomena. Two important observations follow from this figure. Maximum acoustic scattering happens in the vicinity of the shadow direction $\varphi=0$. It is a well-known phenomenon of the forward scattering. Its physical nature is considered in Section 1.5 of Ufimtsev (2014), where it is interpreted as the shadow radiation. This phenomenon is the result of co-phase

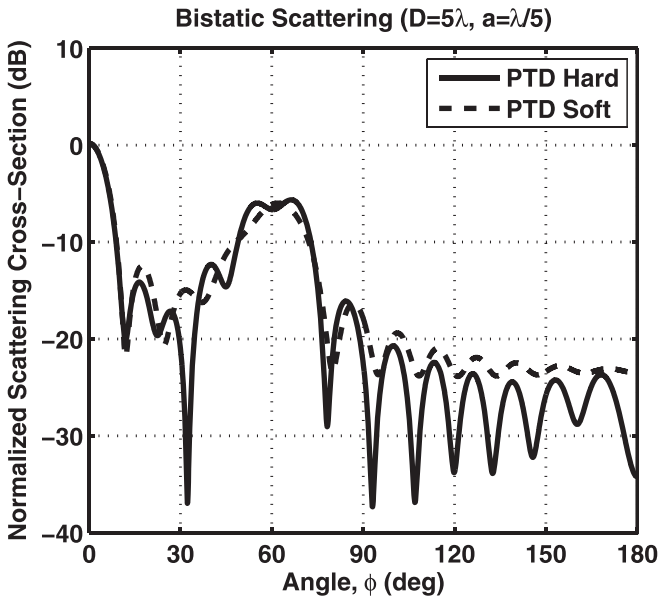

FIG. 6. Bistatic scattering of acoustic waves at the hard and soft rounded trilateral cylinder ($a=\lambda/5, D=5\lambda, dl\cong\lambda/100,\ N_{L_{01}}=N_{L_{02}}=N_{L_{03}}=44, N_{L_1}=N_{L_2}=N_{L_3}=432$).

interference of PO waves in the forward direction that actually represents the focal line for these waves. The second maximum is observed in the vicinity of the direction $\varphi = 60°$ and relates to the specular reflection from the face L_1. The field oscillations are due to the interference of three acoustic edge waves.

The difference between MoM and PTD observed in Fig. 4 is caused by the multiple fringe waves which are absent in this first-order PTD approximation. Their influence becomes noticeably smaller in Fig. 5 for the large cylinder with its size $D = 5\lambda$.

Finally, Fig. 6 demonstrates the scattering of acoustic waves by the hard and soft cylinders where the PTD data for the soft cylinder were reproduced from Apaydin *et al.* (2017b). For large objects, the main lobes generated by the PO currents are actually the same for both cylinders. The difference is observed only in side lobes due to different fringe waves.

V. CONCLUSIONS

The paper provides the extension of PTD for diffraction of acoustic waves at hard finite objects with rounded edges. This extension consists of a combination of the PTD fundamental concept of acoustic fringe currents with the MoM modeling of the currents. In this paper, the rounding shape is chosen as a circular cylinder. It is clear that the developed approach can also be applied to objects with other rounding shapes, as well as for other more complex objects. Comparison of PTD with the exact data reveals a good agreement already in the case when the size of the object is about three to five wavelengths. Hence, for these and longer objects the extended first-order PTD is fully acceptable. Notice also that compared to the exact data found by MoM the developed PTD approach allows one to reduce the computer time approximately by a factor $L/(5\lambda)$. This is the essential advantage of PTD over the direct numeric solutions.

Apaydin, G., Hacivelioglu, F., Sevgi, L., and Ufimtsev, P. Y. (**2014**). "Wedge diffracted waves excited by a line source: Method of moments (mom) modeling of fringe waves," IEEE Trans. Antennas Propag. **62**(8), 4368–4371.

Apaydin, G., Hacivelioglu, F., Sevgi, L., and Ufimtsev, P. Y. (**2016a**). "Fringe waves from a wedge with one face electric and the other face magnetic," IEEE Trans. Antennas Propag. **64**(3), 1125–1130.

Apaydin, G., and Sevgi, L. (**2016**). "The two-dimensional nonpenetrable wedge scattering problem and a Matlab-based fringe wave calculator," IEEE Antennas Propag. Mag. **58**(2), 86–93.

Apaydin, G., Sevgi, L., and Ufimtsev, P. Y. (**2016b**). "Fringe integral equations for the 2-D wedges with soft and hard boundaries," Radio Sci. **51**(9), 1570–1578, https://doi.org/10.1002/2016RS006100.

Apaydin, G., Sevgi, L., and Ufimtsev, P. Y. (**2017a**). "Diffraction at rounded wedges: MoM modeling of PTD fringe waves," Appl. Comput. Electromagn. Soc. J. **32**(7), 600–607, available at http:///www.aces-society.org/includes/downloadpaper.php?of=ACES_Journal_July_2017_Paper_8&nf=17-7-8.

Apaydin, G., Sevgi, L., and Ufimtsev, P. Y. (**2017b**). "Extension of PTD for finite objects with rounded edges: Diffraction at a soft trilateral cylinder," IEEE Antennas Wireless Propag. Lett. **16**, 2590–2593.

Chambers, J. P., and Berthelot, Y. H. (**1994**). "Time-domain experiments on the diffraction of sound by a step discontinuity," J. Acoust. Soc. Am. **96**(3), 1887–1892.

Elsherbeni, A., and Hamid, M. (**1985**). "Diffraction by a wide double wedge with rounded edges," IEEE Trans. Antennas Propag. **33**(9), 1012–1015.

Hallidy, W. (**1985**). "On uniform asymptotic Green's functions for the perfectly conducting cylinder tipped wedge," IEEE Trans. Antennas Propag. **33**(9), 1020–1025.

Hamid, M. (**1973**). "Diffraction coefficient of a conducting wedge loaded with a cylindrical dielectric slab at the apex," IEEE Trans. Antennas Propag. **21**(3), 398–399.

Harrington, R. F. (**1993**). *Field Computation by Moment Methods* (Wiley-IEEE Press, New York), pp. 41–58.

Lucido, M., Panariello, G., and Schettino, F. (**2006**). "Analysis of the electromagnetic scattering by perfectly conducting convex polygonal cylinders," IEEE Trans. Antennas Propag. **54**(4), 1223–1231.

Mitzner, K. M., Kaplin, K. J., and Cashen, J. F. (**1990**). *How Scattering Increases as an Edge is Blunted: The Case of an Electric Field Parallel to the Edge* (Springer, New York), pp. 319–338.

Rozynova, A. M., and Xiang, N. (**2017**). "Secondary surface sources at rigid wedges based on the physical theory of diffraction," J. Acoust. Soc. Am. **141**(5), 3785–3785.

Ufimtsev, P. Y. (**1989**). "Theory of acoustical edge waves," J. Acoust. Soc. Am. **86**(2), 463–474.

Ufimtsev, P. Y. (**2006**). "Improved theory of acoustic elementary edge waves," J. Acoust. Soc. Am. **120**(2), 631–635.

Ufimtsev, P. Y. (**2009**). *Theory of Edge Diffraction in Electromagnetics. Origination and Validation of the Physical Theory of Diffraction* (Revised printing, SciTech Publishing Inc., Raleigh, NC), pp. 45–112.

Ufimtsev, P. Y. (**2013**). "The 50-year anniversary of the PTD: Comments on the PTD's origin and development," IEEE Antennas Propag. Mag. **55**(3), 18–28.

Ufimtsev, P. Y. (**2014**). *Fundamentals of the Physical Theory of Diffraction* (Wiley, Hoboken, NJ), pp. 140–151.

Uslu, M. A., Apaydin, G., and Sevgi, L. (**2014**). "Double tip diffraction modeling: Finite difference time domain vs. method of moments," IEEE Trans. Antennas Propag. **62**(12), 6337–6343.

Vasiliev, E. N., Solodukhov, V. V., and Fedorenko, A. I. (**1991**). "The integral equation method in the problem of electromagnetic waves diffraction by complex bodies," Electromagnetics **11**(2), 161–182.

Xiang, N., and Rozynova, A. (**2017**). "Exploring the physical theory of diffraction for solutions of wedge fields in room-acoustic simulation," J. Acoust. Soc. Am. **141**(5), 3785–3785.

Yarmakhov, G. (**2004**). "Investigation of diffraction of electromagnetic waves at edges of perfectly conducting and impedance wedges with a rounded edge," J. Commun. Technol. Electron. **49**(4), 379 [in Russian: Radiotekhnika I Elektronika **36**(10), 1887–1895 (1991)].